Rapid fabrication strategies for primary and secondary mirrors at Steward Observatory Mirror Laboratory

D. Anderson, H. Martin, J. Burge, D. Ketelsen, S. West
Steward Observatory Mirror Laboratory
University of Arizona
Tucson, Arizona

ABSTRACT

The pursuit of economical fabrication of large (8 m) fast (< f/2), astronomical optics has led to the development of efficient fabrication and testing methods at the Mirror Lab. These methods rely on a mix of advanced technology blended with some traditional practices. Two fabrication strategies have been developed, one or primary mirrors and one for secondary mirrors. Both of these plans rely heavily on the use of the stressed lap both as a grinder as well as for polishing. For secondary fabrication novel methods of testing the convex, severely aspheric mirrors are used.

1. INTRODUCTION

Eight meter class astronomical optics have been a dream of many astronomers since the days of Ritchey and Hale[1]. Sixty years later they are finally becoming realities in a number of projects from various organizations. Fabricating the optics to the required accuracy has driven the fabrication community to adopt novel and powerful techniques to keep the costs of fabrication non-astronomical. The competition between groups has resulted in a diverse array of clever methods. Over the last decade SOML has developed a set of fabrication strategies for very large primary and secondary mirrors, the largest currently slated to be the 8.4 m, f/1.14 primaries for the Large Binocular Telescope (LBT). Not only does the sheer size of these mirrors make them difficult to fabricate but also the very short focal ratios requiring very severe aspheric departures. Requirements for the wavefront quality have only become tighter as the seeing quality is better at many sites. As stepping stones towards fabricating the LBT mirrors the Mirror Lab has fabricated a number of large, fast primaries. These include the 1.8 m, f/1 VATT primary, the 3.5 m f/1.5 SOR primary, and the 3.5 m f/1.75 ARC and WIYN primaries. Currently, the Lab is working on a 6.5 m f/1.25 primary for the MMT and is anticipating a successful casting of its twin for the Magellan Telescope.

Concurrent with the development of primary mirror fabrication methods the Lab is developing new methods for fabricating the very challenging (and numerous) secondary mirrors. Like the primary mirrors, the size and amount of asphericity in these mirrors call for new approaches to testing and fabrication. We have recently developed a new technique for testing these mirrors that will make the fabrication more efficient and accurate.

2. MIRROR BLANK FABRICATION

Primary mirror fabrication begins with the procurement of the blank. The Mirror Lab has developed the capability of making the blanks in the form of a borosilicate honeycomb mirror substrate as shown in Figure 1. All the mirrors mentioned above are of this form. The mirrors are spun-cast to introduce into the blank the required initial curvature. This initial step results in a very large savings in glass and time spent in producing the curvatures, especially at these very low f ratios. Typically, only 6 mm of glass need be removed from the front and rear surfaces to bring them to final thickness.

0-8194-1494-8/94/$6.00

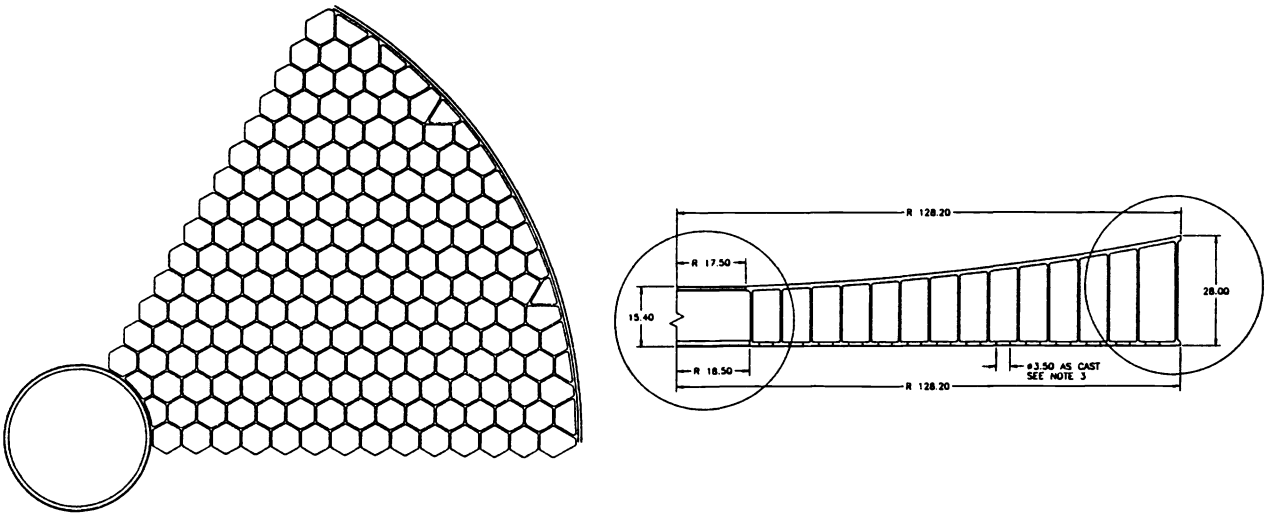

Figure 1. The borosilicate honycomb structure of the 6.5 m cast in the Mirror Lab's spinning furnace.

3. PRIMARY MIRROR FABRICATION STRATEGY

Experience gained in fabricating the 3.5 m mirrors and the 1.8 m f/1 mirror has enabled us to converge on a fabrication strategy that is very efficient as well as capable of producing very high quality surfaces. While some details of the plan are related specifically to borosilicate or honeycomb mirrors, the basic strategy can be applied to any large optic.

The development of the strategy follows from the optical surface requirements for the mirrors. For these ground-based telescopes a structure function has been adopted that follows from wavefront propagation through the atmosphere.[2] The structure function defines the required figure quality in terms of rms wavefront (or surface height) differences over a spectrum of spatial scales ranging from less than a centimeter up to the full aperture of the mirror. In Figure 2 is a plot of the required structure function for the LBT mirrors. Like the atmospherically distorted wavefront, the mirror figure must be much more accurate at small scales than large scales. The limiting small scale accuracy requirement (5 nm rms surface error) is set by the requirement that no more than 3% of the light at a wavelength of 350 nm be scattered outside the seeing disk.

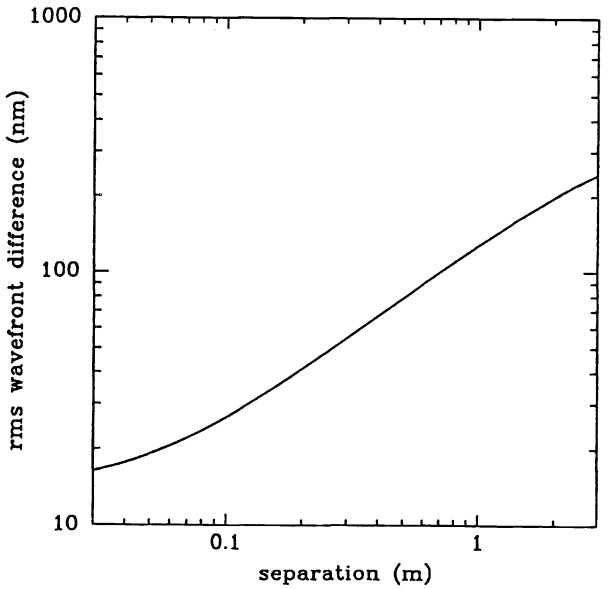

Figure 2. The structure function specification for the LBT primary mirror.

Given this form of the specification it is clear that it is important to produce a surface that is as smooth as possible at small spatial scales where the spec is very tight. At large spatial scales the requirement is considerably relaxed which suggests fabrication methods that produce smooth surfaces but may have more difficulty with large scale errors. As will be seen from our results, with the methods that we employ, when the spec is achieved at small scales the large scale errors are many times better than required. The strategy that has emerged from our work is shown schematically as:

Fixed diamond generate asphere. Profilometry with LVDT on LOG. ⇒ Stressed lap grind with loose abrasive. IR interferometry ⇒ Stressed lap polish ⇔ Small tool correction Visible interferometry

It is vitally important in rapid fabrication that each process step avoid introducing errors that cannot be rapidly removed by subsequent steps. One key element of this is to properly support the optic throughout the process that in a way closely duplicates the final support and does not imprint any errors during the polishing process. For this reason a "polishing cell" for each mirror is constructed that duplicates the telescope cell support forces as closely as possible. The mirror is installed on this support prior to work on the optical surface. This support is a passive hydraulic system of interconnected rolling diaphragm actuators delivering a support that duplicates the axial support of the active supports in the telescope cell.

3.1 Fixed diamond generation.

The first step in the process is the removal of a nearly uniform thickness layer of glass from the surface to achieve final faceplate and backplate thickness while at the same time introducing the asphere. This is done with fixed diamond tools working on the Large Optical Generator (LOG).[3] This machine can be rapidly configured for either generating or grinding/polishing with either a passive or active lap. For generating, the machine is capable of generating up to 8.4 m aspheres to 10 microns rms.

Initial generating is performed with a coarse diamond cup wheel to remove about 6 mm of glass on the front and backplates to bring them to the desired thickness. While the machine can remove up to 17 cubic inches of glass per minute we typically remove about 8 cubic inches per minute. Following the rough removal, two sizes of fine diamond, 220 mesh and 600 mesh, in a resin bond cup wheel, are used to give the surface a smooth finish with low subsurface damage. While we have demonstrated that this surface can be directly polished the remaining figure errors are large enough that lapping the surface with loose abrasive is much more efficient.

To monitor the figure during aspherization the surface is profiled *in situ* with an LVDT mounted on the LOG spindle. In this way errors due to wheel geometry and wheel wear as well as setup errors can be removed. In addition, azimuthal measurements can be made to check the functioning of the support and turntable. Corrections can be made directly in the tool path profile to reduce the surface errors. The limitation on the figure quality at this stage is largely the calibration accuracy of the machine.

3.2. Stressed lap grinding

Loose abrasive lapping of the surface, while not as rapid as generating with diamond, is much more easily controlled. Since a fine surface has already been achieved through fine diamond generating, removal of figure errors is now the main concern. The lapping is accomplished with the stressed lap[4,5], where the pitch layer is coated with a thin layer of zinc.

Use of the stressed lap grinder/polisher is the key element in the rapid figuring of the mirror. The basic strategy of using the stressed lap is to use a tool that is large enough to smooth the surface rapidly but small enough to be useful in correcting figure errors. The lap is actively deformed under computer control so that the lap always closely fits the aspheric shape of the mirror. This provides for rapid smoothing of already rough surfaces and, once smooth, does not introduce high frequency zonal errors common with passive laps. The lap that has been used for the 3.5 m mirrors will also be used on the 6.5 m and 8.4 m mirrors. It is 1.5 m in diameter with a maximum pitch

surface 1.2 m in diameter. The lap, shown in cross section in Figure 3, is composed of a 1.5 m diameter, 50 mm thick plane parallel aluminum plate with a layer of nylon that is shaped to provide the minimum lap curvature. Actuators apply bending moments to the plate to provide a variable increase in curvature and other low order deformations. The nylon is faced with a layer of pitch for polishing and an additional thin layer (.4 mm) of zinc for grinding.

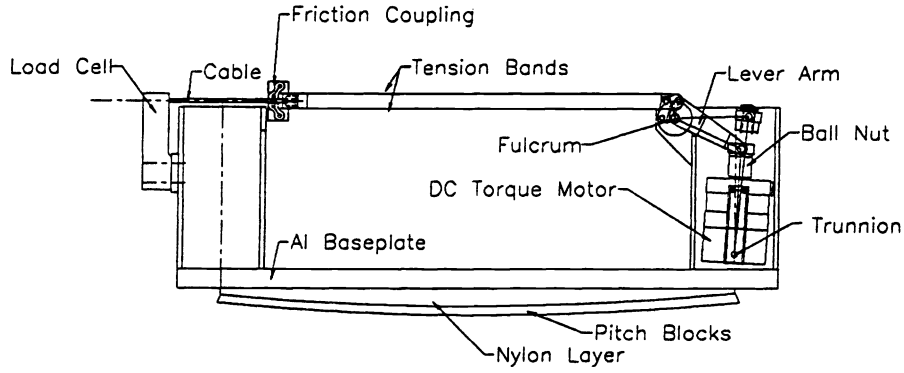

Figure 3. Cross sectional view of the stressed lap.

The stressed lap grinder can very rapidly remove the very high frequency errors created by the diamond wheel during generation. In a matter of a few hours the surface is smooth enough to use IR phase measuring interferometry to monitor the surface figure. In the case of the WIYN primary mirror, the f/1.75 asphere (170 microns from best fit sphere) was completely ground in with the stressed lap grinder and loose abrasive. By gradually increasing the amount of bending in the lap from no bending (when the mirror is spherical) to that required by the full asphere, the asphericity was introduced in a very smooth fashion. The mirror was fully aspherized in this way in less than five weeks work and 52 hours of machine time. The working size of the lap was chosen at .8 m to efficiently introduce the asphere from the best fit sphere by working only on the center and edge and very little on the .7 zone. It is clear from Figure 4 how smooth this process was.

(a) (b)

Figure 5. In (a) is an IR interferogram of the WIYN mirror after 10 hours of grinding. In (b) is shown an IR interferogram at the end of grinding through the null lens.

The lap size was large enough to prevent the creation of high frequency radial zones but small enough to remove any mid-frequency zonal errors by the proper choice of the polishing stroke. The machine operates under computer control via control software where lap stroke parameters such as the rotational speeds of the lap and mirror, the

extent of the stroke, and the stroke velocity are all controlled. These many degrees of freedom available in the design of a stroke gives wide latitude in the spatial extent of the wear. These degrees of freedom are illustrated in Figure 5. Polishing pressure can also be controlled dynamically to address non-axisymmetric figure errors, and the system will soon include dynamic control of moments corresponding to pressure gradients across the lap.

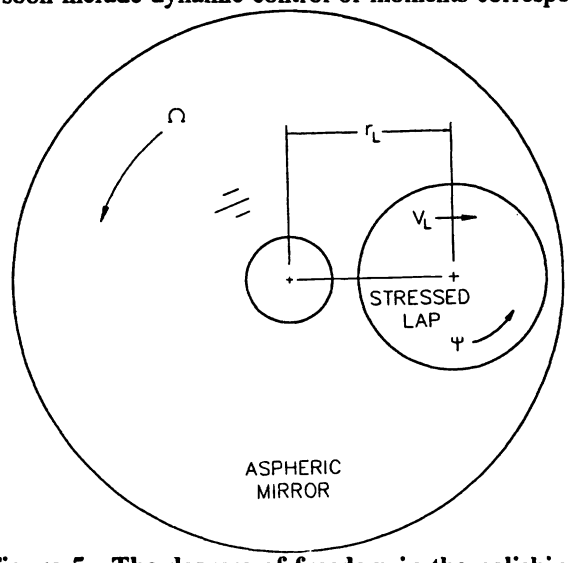

r_{in}, r_{out}	Extents of stroke
$\psi(\Omega, r_L)$	Lap rotation rate
$v_L(\Omega, r_L)$	Lap linear velocity
ΔK	Effective misfit in the conic constant
T	Polishing time

Figure 5. The degrees of freedom in the polishing stroke using the stressed lap.

Predictive software[6] provides guidance on the utility of any stroke in removing radial errors prior to a polishing run. Convergence can be very rapid with improvements in the figure by a factor of 2 per week. Shown in Figure 6 are average radial profile plots of predicted and actual removal for a polishing run made during the polishing of the SOR 3.5 m primary. The removal, in this case, closely matches that predicted by the predictive software. The predictions made are not always so close to the actual removal. Other factors influencing the wear such as lap misfit and the constantly changing condition of the pitch, result in less deterministic wear. There is still a large measure of empirical selection of stroke paramenters based on wear results from similar stroke parameters. The Lab is about to initiate a full set of controlled experiments on a 1.8 m mirror on a smaller polishing machine to improve the predictions leading to even more rapid convergence.

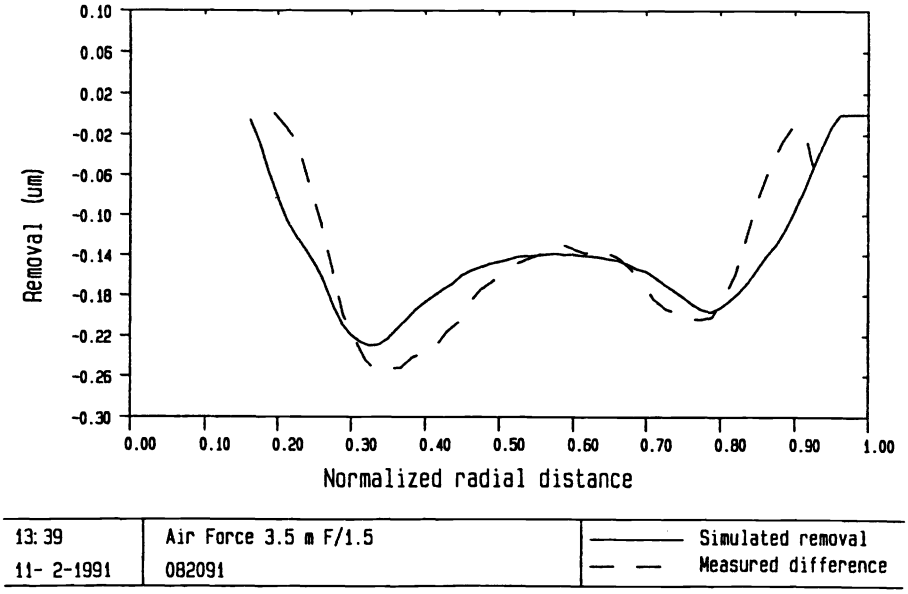

Figure 6. Average radial profile plots comparing actual removal to the predicted removal during a polishing run with the stressed lap.

When about 20 microns of glass have been removed from the surface and figure errors are below 1 micron rms polishing commences. We try to improve the surface figure even during the initial polishing when the primary goal is to completely polish the surface. By combining the polish-out stage with some figuring we are able to converge rapidly to a surface that is about .25 microns rms and polished out.

Phase measuring IR interferometry guides the process through the grinding stage and into the initial polishing stage. A germanium null lens provides correction for the asphericity. It is critical for rapid convergence to final figure that this null lens be made as accurately as possible. Computer-generated holograms will be used to verify the accuracy of both the IR null lens and the visible null lens.[7] By certifying both null lenses with the hologram any errors detected in their construction can be mapped and removed from the data assuring an accurate test.

3.3. Final figuring.

At this point we switch to visible phase measuring interferometry through a null lens and proceed with the final figuring with the stressed lap. The phase map of the surface provides us with a very detailed surface error map. Three types of surface error are addressed in different ways. The surface can be thought of as a sum of purely radial errors, low order azimuthal errors (such as astigmatism) and high frequency azimuthal errors (small bumps and holes). Low order azimuthal errors are addressed by active control of the pressure the lap exerts on the glass because the polishing rate varies approximately linearly with the lap pressure. A "pressure map" is generated from the phase data and the polishing stroke parameters, and is used to vary the pressure during the polishing run. The large scale azimuthal errors are very quickly controlled in this way.

Azimuthal errors on the order of the size of the lap are not readily removed by pressure variations. There is a great deal of natural smoothing that occurs but some degree of this type of error remains. There are two ways we can remove them. The first is to provide a pressure gradient across the lap that can better resolve the polishing forces and hence the removal. This is done by using three tilt actuators attached to the lap that can apply moments to the lap creating pressure gradients across it. This can provide more localized polishing and better removal of the azimuthal errors and radial errors as well. The second method is to use a small passive tool (about 200 mm diameter) on an orbital spindle attached to the main spindle, and under constant pressure simply use increased dwell time over the high areas to rapidly converge. While small tool polishing is efficient in removing this type of error we use it sparingly since it does tend to introduce very high frequency errors. Fortunately, the stressed lap is very efficient at removing that type of error so we alternate between them when using the small lap.

The remaining radial errors are removed by the selection of the proper stroke parameters. High frequency errors are smoothed by the well fitting lap leaving only mid to low frequency radial errors. Pressure gradients across the lap can reduce the spatial frequency of the removal as can simply making the lap smaller in size.

One of the difficulties faced with any lightweight honeycomb or cellular mirror is the "print-through" of the cellular structure of the mirror into the surface figure during polishing. The problem originates when the lap passes over the unsupported area between the ribs which deflect under the lap pressure thus reducing the polishing force and the wear. After the lap passes by, the core areas spring back and appear as bumps in the surface. In Figure 7 is a phase map of the WIYN mirror during the initial stage of polishing when the polishing pressures used were high (.5 psi). The bumpy pattern on the surface is the print-through of the cellular structure. The accompanying contour plot is of the "average cell" showing the shape and magnitude of the average print-through. To reduce this effect the mirror is internally pressurized with air during polishing. The pressure is adjusted to be the same as the average lap polishing pressure, which supplies just enough force to balance the lap pressure to produce near zero deflection of the surface. In Figure 8 is shown a phase map of the finished WIYN mirror and a plot of the average cell. The stressed lap has removed the existing print-through and reduced the remaining error by a factor of 7. The remaining print-through at 6 nm p-v is negligible with respect to the structure function specification. The pressurization of the mirror does cause some low order bending of the mirror (about .6 waves of astigmatism) but the stressed-lap is small enough to ride over the low order error without imprinting it into the surface. When the pressure is turned off for testing the error vanishes.

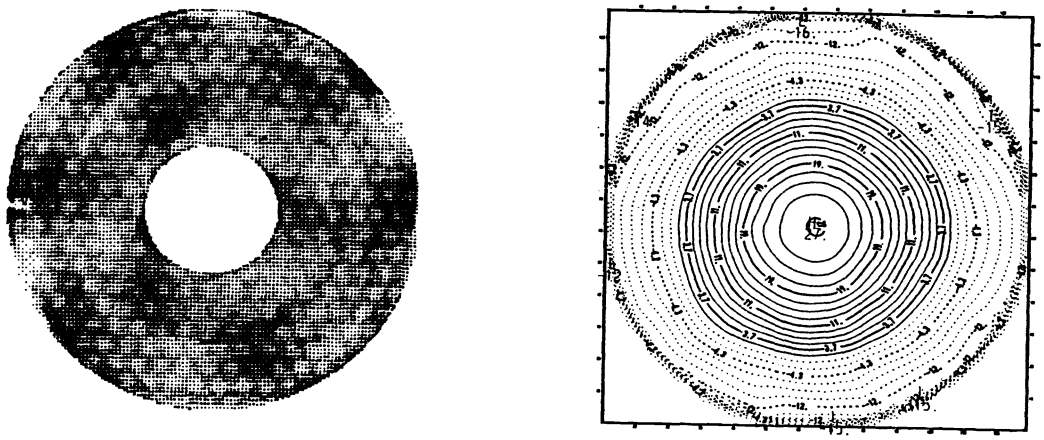

Figure 7. The print-through resulting from unbalanced polishing forces over the cellular structure.

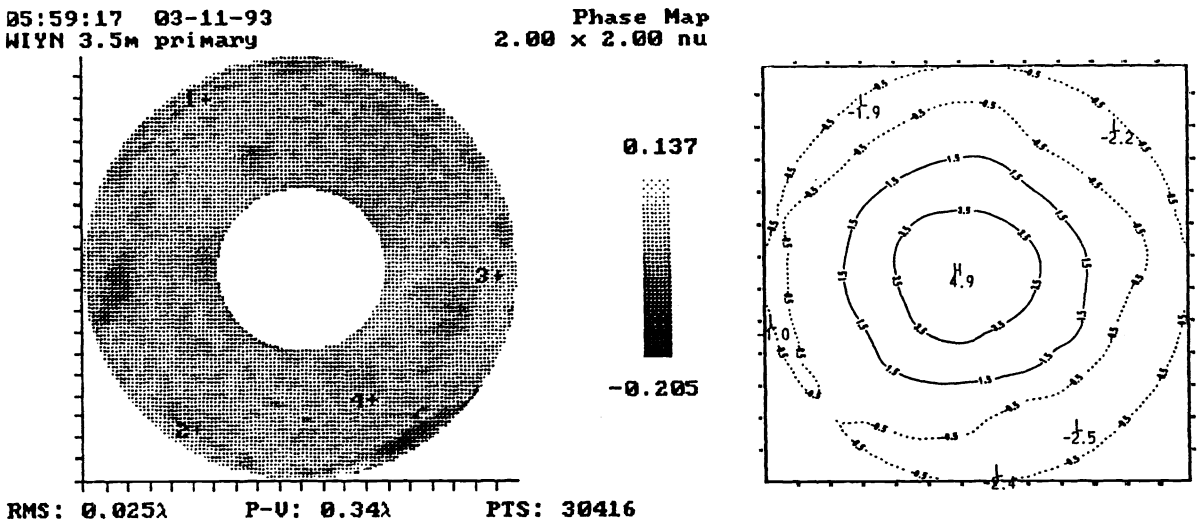

Figure 8. When the polishing force over the cells is balanced by air pressure there is almost complete removal of the print-through.

3.3. Results of the process.

In Figure 9 is a plot of the convergence of the WIYN primary mirror from a sphere to the final figure[8]. Also shown is the final surface map of the mirror in Figure 10 and the structure function plotted along with the specification in Figure 11. The entire aspherizing process took only 21 weeks and only 100 hours of total machine time, including 9 weeks of polishing the ground surface.

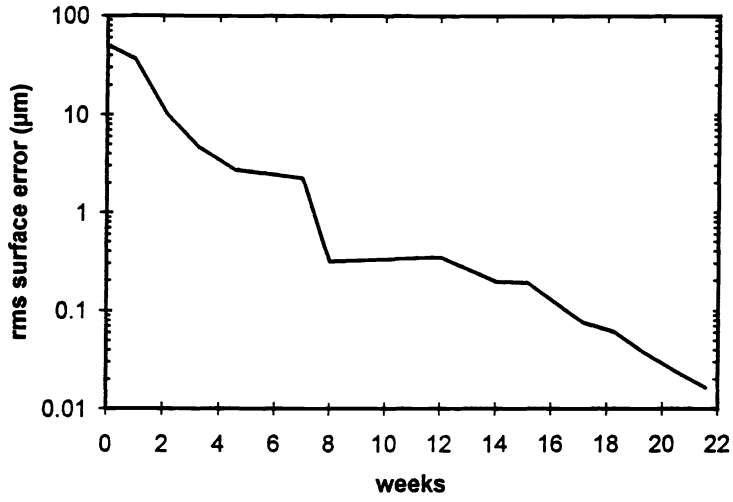

Figure 9. The convergence to final figure for the WIYN primary.

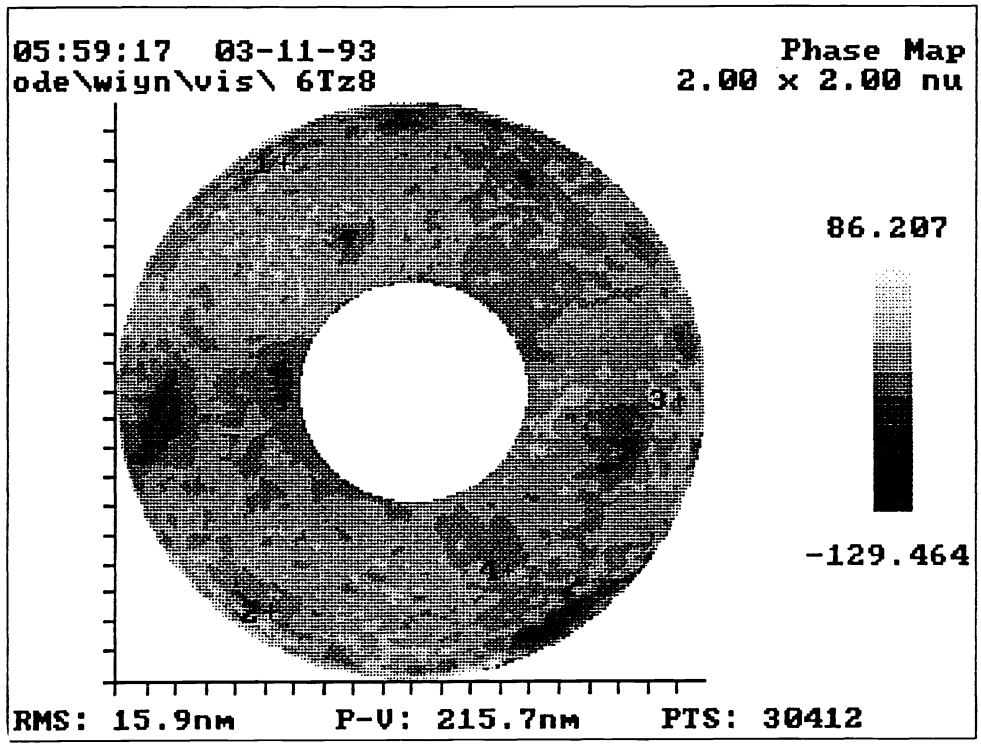

Figure 10. The final phase map of the WIYN primary mirror over the clear aperture with a small amount of residual astigmatism removed.

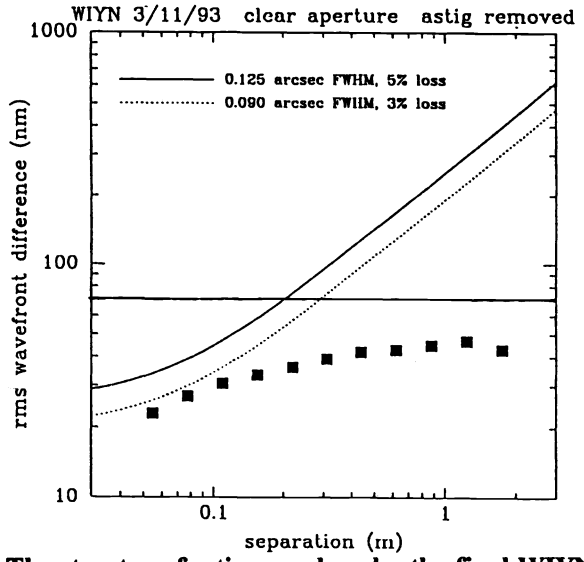

Figure 11. The structure funtion produce by the final WIYN surface.

For future mirrors beginning with the 6.5 m MMT primary we will have the advantage of using the results of the polishing experiments to improve convergence as well as guide the use of pressure gradients to control the wear.

4. SECONDARY MIRROR FABRICATION STRATEGY

4.1. Introduction.

Shown in Table 1 is a list of secondary mirrors currently scheduled to be made by the Mirror Lab. They are for three projects: the MMT 6.5 m upgrade, the Sloan Digital Sky Survey Telescope, and the LBT. They range in size from .6 m to 1.6 m, and though small, are numerous and highly aspheric so rapid fabrication methods are required.

	Sloan	MMT *f*/9	MMT *f*/15	MMT *f*/5	LBT *f*/15	LBT *f*/4
Diameter (mm)	1143	996	620	1653	872	1170
Radius of curvature (mm)	7194	2806	1663	5022	-1890	3294
Conic constant	-12.110	-1.749	-1.397	-2.640	-0.733	-3.236
Surface sag (mm)	22.7	44.2	28.9	68.0	-50.3	51.9
P-V asphere (microns)	108.4	152.2	87.7	304.0	-122.5	331.4
focal ratio	3.15	1.41	1.34	1.52	-1.08	1.41

Table 1. Secondary mirrors scheduled to be fabricated at the Mirror Lab.

The secondary mirror fabrication strategy is centered more fully around the stressed lap since there will be no fixed diamond generation of the asphere into the surface. The lapping in of the asphere on the WIYN primary was so successful that we will use that as the aspherization method. Prior to aspherizing the mirrors they will first be generated and ground to a radius of the best-fit sphere using a full sized tool in conventional fashion. For aspherizing the mirrors the basic fabrication strategy is as follows:

Stress-lap grind asphere with loose abrasive. Test *in-situ* with swing-arm profilometer. ⇒ Stress-lap polish asphere. ⇔ Small tool correction ⇒ Test with full-sized holographic test plate

4.2. Stressed lap grinding of the asphere and swing-arm profilometry.

As described above, the stressed lap will be used as a grinding tool to lap in the asphere with loose abrasives. The shape of the lap will be varied with the amount of asphere as the process progresses so that the lap always fits the surface reasonably well. When the mirror is about 90% aspherized polishing will commence.

Monitoring the aspherization with IR interferometry is difficult to do with convex aspheres of the sizes and speeds required. Instead, we will use a swing-arm profilometer[9,10] to measure the mirrors *in-situ* on the polishing machine. In swing-arm profilometry an arm holding an LVDT (as shown in Figure 12) is turned about an axis that intersects the axis of the mirror at its center of curvature. When this is the case and the indicator passes through the center of the mirror, the indicator will measure the aspheric departure of the mirror. The tilted arm removes the spherical component of the surface. This is the same principal used in curve generating spheres with diamond cup wheels. The profilometer will enable us to aspherize the mirror to about the same level as IR interferometry, around .3 microns rms. Unlike IR interferometry, however, only a radial profile is produced, not a full surface map. We expect that the azimuthal errors introduced by the stressed lap grinding will be small and could be removed in final figuring.

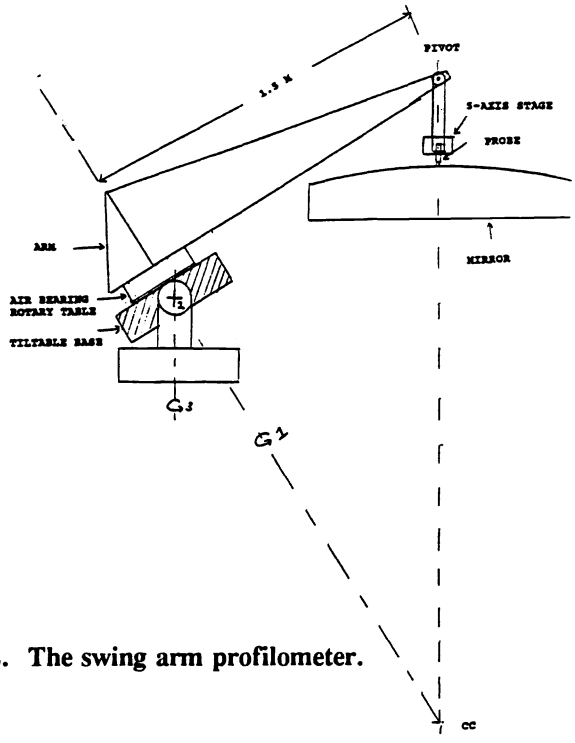

Figure 12. The swing arm profilometer.

4.3. Optical testing.

Following aspherization and initial polishing of the surface, final figuring will be performed with the stressed lap guided by a novel test method--a holographic test plate.[11] Secondary mirrors have in the past been tested by

a variety of methods including the Hindle test, the Hindle shell test, through the rear surface with a null lens, with an aspheric test plate, and simply in the telescope. We will use a variation of the aspheric test plate method. In this method an aspheric test plate is made that is the exact opposite match of the surface of the secondary. When the surfaces are brought into proximity and properly illuminated, fringes are formed that show the difference between the two surfaces. The better the test plate surface is made and measured independently the better the secondary surface is known. This test has the advantage that there is only one precision surface required, the reference surface itself. The illumination and imaging optics can be of lower precision. Since the two surfaces are in close proximity to one another (a few millimeters separation) environmental errors from vibration and seeing are negligible. Unfortunately, the reference surface is also an asphere and for these fast systems a very challenging task to make and certify.

To get around this problem we use a spherical test plate, which is easy to make and certify, and on its surface write a hologram that by diffraction provides the aspheric portion of the test beam. It is identical to a standard test plate configuration with the aspheric test plate surface replaced with a spherical surface with a hologram written on it. Alignment of the system is identical to that of an aspheric test plate and is guided by the fringes in a straightforward way.

For rapid testing the holographic test plate is fixed in a mount adjacent to the secondary polishing machine as shown in Figure 13. To test the secondary mirrors as they will be used in the telescope, i.e., upside down, the mirror will be polished in an invertible cell. The mirror and cell will be picked up off the polishing machine, inverted, and then set down on kinematic mounts just above the test plate. The test plate support ring will itself be supported at three points driven by PZT actuators to provide phase measuring capability. This test will provide a rapid, full aperture measurement of the secondary that will be used to guide the figuring.

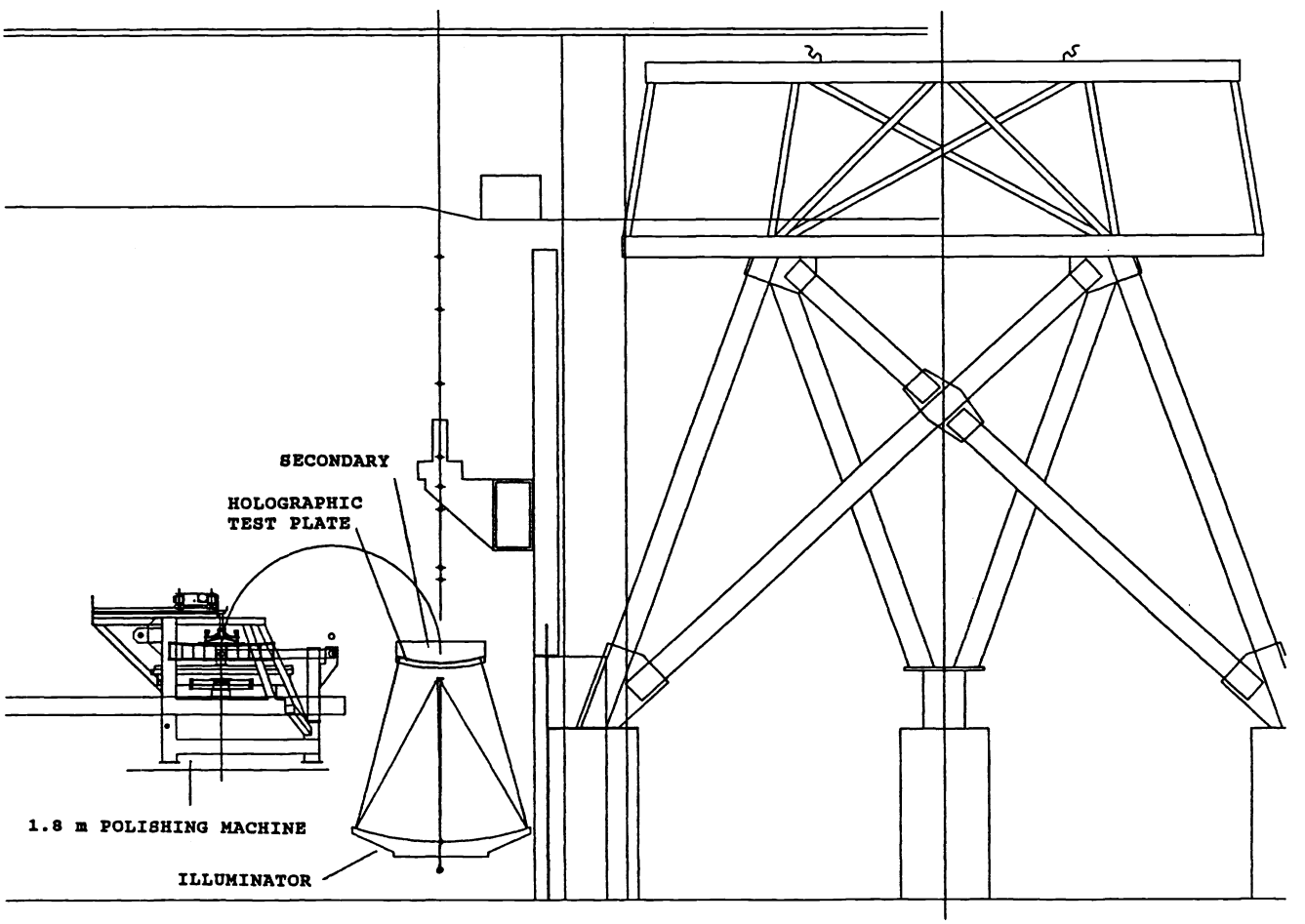

Figure 13. A flipping mechanism will deliver the inverted secondary into position for holographic testing.

3.3. Final figuring.

Final figuring will be done with the same lap control system as the primary mirrors. Stroke control will remove the radial errors and a combination of pressure variations and pressure gradients will remove the azimuthal errors. Small tool polishing will, again, be sparingly used as required to touch up the local errors, followed by stressed lapping. Given the relatively large size of these mirrors most of them will be cellular mirrors. Like the primaries, they will be pressurized during polishing to remove the print-through.

Since the mirrors will be tested full aperture to high resolution in the same support in which they will be used, we expect rapid convergence to final specification and very high quality images in the telescope.

REFERENCES

1. D.E. Osterbrock, *Pauper & Prince,* The University of Arizona Press, 1993

2. J.M. Hill, "Optical Design, error budget, and specifications for the Columbus Project Telescope." SPIE Vol. 1236, *Advanced Technology Optical Telescopes IV,* 1990

3. D. Ketelsen, W. Davison, S. DeRigne, W. Kittrell, "A machine for complete fabrication of 8-m class mirrors.", SPIE Vol. 2199, *Advanced Technology Optical Telescopes V,* 1994 (in press).

4. H.M. Martin, D.S. Anderson, J.R.P. Angel, R.H. Nagel, S.C. West, and R.S. Young, "Progress in the Stressed lap polishing of a 1.8 m f/1 mirror", *Advanced Technology Optical Telescopes IV,* SPIE Vol 1236, 1990.

5. H.M. Martin, D.S. Anderson, J.R.P. Angel, J.H. Burge, W.B. Davison, S.T. DeRigne, B.B. Hille, D.A. Ketelsen, W.C. Kittrell, R. McMillan, R.H. Nagel, T.J. Trebiski, S.C. West, and R.S. Young, "Stressed lap polishing of 1.8-m f/1 and 3.5-m f/1.5 primary mirrors.", *Proc. ESO Conference on Progress in Telescope and Instrumentation Tecnologies,* ed. M.H. Ulrich, 1992.

6. J.H. Burge, "Computer simulation and optimization of stressed lap polishing.", *OSA Annual Meeting Technical Digest,* 1990.

7. J.H. Burge, "Certification of null correctors for primary mirrors," *Advanced Optical Manufacturing and Testing IV,* SPIE Vol. 1994, 1993.

8. D. Anderson, J. Burge, D. Ketelsen, B. Martin, S. West, G. Poczulp, J. Richardson, W. Wong, "Fabrication and testing of the 3.5 m f/1.75 WIYN primary mirror," SPIE Vol 1994, *Advanced Optical Manufacturing and Testing IV,* 1993.

9. D.S. Anderson, R.E. Parks, L. Shao, "Versatile Profilometer for Aspheric Optics", *Optical Fabrication and Testing Technical Digest,* Vol 11, 1990.

10. D.S. Anderson, "Swing-arm Profilometer", Mirror Lab Technical Memo, February, 1994.

11. J.H. Burge, D.S. Anderson, "Full-aperture interferometric test of convex secondary mirrors using holographic test plates", *Advanced Technology Optical Telescopes V.,* SPIE Vol 2199, 1994 (in press).